

TREND

Trapped Radiation Environment Model Development

Time Dependent Radiation-Belt Space Weather Modelling

ESA/TOS-EMA Contract No. 11711/95/NL/JG - CCN 1 to Work Order No. 3

Technical Note 1A

Short review of the electron database subsets

D. Heynderickx
(July 1998)

B.I.R.A. – I.A.S.B.	D.E.R.T.S.	P.S.I.
Avenue Circulaire 3 B-1180 Brussel Belgium	ONERA CERT BP 4025 F-31055 Toulouse cedex 4 France	Laboratory for Astrophysics CH-5232 Villigen Switzerland

Short review of the electron database subsets

The Salammbô simulations in this study require as boundary values measurements of the particle population in the geostationary region. Therefore, the first step in this study was to identify periods of interest during which data from geostationary satellites are available, as well as data obtained in the inner part of the radiation belts in order to evaluate the results of the Salammbô code.

This Part of Technical Note 1 describes the data sets that were used for the Salammbô study and the selection process that resulted in a set of case studies.

1.1 Overview of the spacecraft suitable for the study

1.2 Selection of the periods of interest

References

List of figures

1.1 Overview of the spacecraft suitable for the study

During the previous TREND studies, electron data from instruments on four satellites have been obtained: CRRES/MEA, Meteosat/SEM-2, ISEE-1/WIM and ISEE-2/KED. In the framework of the current study, the MIR/REM and STRV/REM data have been delivered as well. Finally, for the SPENVIS project (<http://www.spennis.oma.be>) the complete set of GOES/SEM data has been downloaded to BIRA/IASB. Figure 1.1 shows the time coverage of the respective missions.

1.1.1 The GOES/SEM spacecraft and instruments

1.1.2 The Meteosat-3/SEM-2 spacecraft and instrument

1.1.3 The CRRES/MEA spacecraft and instrument

1.1.4 The STRV1b/REM spacecraft and instrument

1.1.5 The MIR/REM spacecraft and instrument

1.1.6 ISEE-1 And ISEE-2

1.1.1 The GOES spacecraft and instruments

1.1.1.1 GOES 5-7

GOES 5-7 were a series of NASA-developed, NOAA-operated, geosynchronous, and operational spacecraft. The spin-stabilized spacecraft carried (1) a Visible/Infrared Spin-Scan Radiometer (VISSR) Atmospheric Sounder (VAS) to provide high-quality day/night cloudcover data, to take radiance-derived temperatures of the Earth/Atmosphere system, and to determine atmospheric temperature and water vapor content at various levels, (2) a meteorological data collection and transmission system to relay processed data from central weather facilities to APT (Automatic Picture Transmission)-equipped regional stations and to collect and retransmit data from remotely located Earth-based platforms, and (3) a Space Environment Monitor (SEM) system to measure proton, electron, and solar X-ray fluxes and magnetic fields. The cylindrically shaped spacecraft measured 190.5 cm in diameter and 230 cm in length, exclusive of a magnetometer that extended an additional 83 cm beyond the cylindrical shell. The primary structural members were a honeycombed equipment shelf and thrust tube. The VISSR telescope was mounted on the equipment shelf and viewed the Earth through a special aperture in the side of the spacecraft. A support structure extended radially from the thrust tube and was affixed to the solar panels, which formed the outer walls of the spacecraft to provide the primary source of electrical power. Located in the annulus-shaped space between the thrust tube and the solar panels were stationkeeping and dynamics control equipment, batteries, and most of the SEM equipment. Proper spacecraft attitude and spin rate (approximately 100 rpm) were maintained by two separate sets of jet thrusters mounted around the spacecraft equator and activated by ground command. The spacecraft used both UHF-band and S-band frequencies in its telemetry and command subsystem. A low-power VHF transponder provided telemetry and command during launch and then served as a backup for the primary subsystem once the spacecraft had attained synchronous orbit.

The implemented data set consists of averaged SEM electron measurements.

The energetic particle monitor consisted of three detector assemblies, each covering limited regions of the overall energy spectrum. The first two detector assemblies monitored protons in seven energy ranges between 0.8 and 500 MeV and alpha particles in six energy ranges from 4 to >400 MeV. There was also one channel for the measurement of electrons in the energy range above 500 keV. The third detector, High Energy Proton and Alpha Detector (HEPAD), monitored protons in four energy ranges above 370 MeV and alpha particles in two energy ranges above 640 MeV/nucleon. In all, there were 25 channels of data, each channel sampling at a slow rate of once in a few seconds, or once in a few minutes.

GOES 5

Goes 5 was the seventh satellite of the series. On July 30, 1984, GOES 5 VAS experienced a failure, thus NOAA was prompted to relocate GOES 6 to a more central 98 deg W position, and to reactivate GOES 1 and GOES 4 for the acquisition and relay of VISSR information, respectively, from the western United States.

The 5-minute averaged GOES-5/SEM electron data (>2 MeV) cover the period 01/1986 - 03/1987.

GOES 6

GOES 6 was the eighth satellite in the series. GOES 6 was moved from its 135 deg W position to a more central 98 deg W position when GOES 5 failed on July 29, 1984. It was turned off on November 12, 1994.

The 5-minute averaged GOES-6/SEM electron data (>2 MeV) cover the period 01/1986 - 11/1994.

GOES 7

GOES 7 was the tenth satellite in the series. The 5-minute averaged GOES-6/SEM electron data (>2 MeV) cover the period 01/1986 - 11/1994.

1.1.1.2 GOES 8

GOES 8 is the 11th in a series of NASA-developed, NOAA-operated, geosynchronous and operational spacecraft. The triaxis-stabilized spacecraft carries (1) Imager and Sounder system to provide visible and infrared images of cloud cover, and to determine atmospheric temperature and water vapor content at various levels, (2) a meteorological data collection system to relay processed data from central weather facilities to regional stations equipped with APT and to collect and retransmit data from remotely located earth-based platforms, (3) a Space Environment Monitor (SEM) system to measure proton, electron, and solar X-ray fluxes and magnetic fields, (4) a Search And Rescue (SAR) system to detect and relay distress calls from land and ocean, and (5) a WEFAX system to disseminate weather information to the user community via FAX. The cylindrically shaped spacecraft measures 190.5 cm in diameter and 230 cm in length, exclusive of a magnetometer that extends an additional 300 cm beyond the cylindrical shell. The imaging telescope is mounted on the equipment shelf and views the earth through a special aperture in the side of the spacecraft. The solar array of 1,057 W supplies two nickel-cadmium batteries of 12 Ah each. The CCSDS (Consultative Committee for Space Data Systems) -compliant telemetry is in real-time at 2.0 kbs through S-bands. The eventual parking longitude of the spacecraft will be over 75 deg W.

The energetic particle sensor consisted of three independent detectors: (1) EPS Telescope, (2) Dome Assembly, and (3) High Energy Proton and Alpha Detector (HEPAD). EPS telescope operated on the $dE/dX - E$ mode, each of the detectors being a surface barrier semiconductor; pulse height analysers could identify a particle either as a proton or as an alpha, besides binning them into narrower energy ranges. The Dome detector carried three separate windows of differing thicknesses, behind which lay a pair of 1500 micron thick surface barrier silicon detectors. Outputs from this three pairs of detectors passed through pulse height analyzers to provide counts in narrower bands. HEPAD is a Cerenkov counter, backed by pulse height analyzers. Over all, there were 11 energy channels for protons, eight for protons (?alpha particles?), and one for electrons of energy >2 MeV. However each such channel carried nontrivial contamination by other species. The counts from each of the 20 channels were accumulated for a few seconds (3 to 12 seconds, depending on the channel) before sampling the accumulated total for telemetry. There were also saturation limits to the level of accumulated counts, varying from 1,200 to 25,000 counts, depending upon the channel. The proton and Alpha channels covered the energy range of several hundred keV to several hundred MeV.

The 5-minute averaged GOES-8/SEM electron data (>2 MeV) cover the period 03/1986 to the present.

1.1.1.3 GOES 9

The Geostationary Operational Environmental Satellite (GOES-J) is the second satellite in a series of next generation geosynchronous spacecraft, referred to as GOES-NEXT and represented by the GOES I through GOES M spacecraft. The GOES-NEXT series is a joint effort on the part of NASA and NOAA to provide continued operational monitoring of weather systems primarily over the United States, distribute meteorological data to regional and national weather offices within the USA, contribute to the development of an environmental data collection network, contribute to the search and rescue program, improve the capability for forecasting and provide real-time warnings of solar disturbances, and to extend knowledge and understanding of atmospheric processes to improve short and long-term weather forecasts. The GOES-NEXT series, extends the capabilities of the previous GOES 1-7 spacecraft. The GOES I-M spacecraft will be placed over the equator at 135 deg West or 75 deg West. The spacecraft structure is based on the Space Transportation System (STS)-launched, three-axis stabilized Insat (geostationary satellite for India) meteorological satellite design. The design allows unobstructed views of the Earth for operational coverage by the spacecraft sensors. The spacecraft configuration is a compact box-shaped main body that carries the Earth-observing instruments, a continuous-drive solar array attached to the south panel through a yoke assembly, and a solar pointing instrument gimbal mounted on the solar panel yoke. The main body accommodates the sensors, electronics, and support subsystems. The communication antennas, except the Tracking, Telemetry, and Command (TT&C) antenna, are hard-mounted to the Earth-facing panel. The Propulsion Module consists of the fuel and oxidizer tanks for the bipropellant propulsion subsystem mounted on the central cylinder. The Attitude and Orbit Control Subsystem (AOCS) provides attitude control of the spacecraft. The AOCS consists of the sensors, electronics, and the actuators. The GOES power is generated from the solar array and two 12 Ah batteries. Power is automatically regulated during solar eclipses. The Image Navigation/Registration (INR) system provides Imager and Sounder data products in real-time to users. The Communications, Command, and Data Handling subsystem is comprised of antennas, receivers, transponders, transmitters, data encoders and encryptors and multiplexers. The Tracking Telemetry and Command (TT&C) subsystem provides the necessary monitor and command link between the spacecraft and the ground stations. The GOES-NEXT instruments consist of the following: (1) Earth Imaging System, a 5-channel visible and infrared radiometer which provides Earth imagery 24 hours a day; (2) Sounding System, a 19-channel discrete-filter radiometer for

obtaining atmospheric temperature and moisture soundings; (3) a Space Environment Monitor (SEM), which consists of a magnetic field sensor, a solar X-ray sensor, an Energetic Particle Sensor (EPS), and a High Energy Proton and Alpha Detector (HEPAD); (4) a Search and Rescue subsystem (SARSAT), which receives signals from 406 MHz distress beacons and relays them to the ground; (5) a Data Collection System (DCS) for collecting and relaying real-time information from Data Collection Platforms (DCPs) such as buoys, balloons, remote weather stations, ships, and aircraft; and (6) a Weather Facsimile (WEFAX) system which relays processed weather imagery from the Wallops Island station to the user community.

The Space Environment Monitor (SEM) System on the GOES-NEXT series of geostationary meteorological satellites (GOES-I through GOES-M) is designed to provide direct real-time measurement of solar activity. The SEM consists of a Magnetic Field Sensor, a Solar X-ray Sensor, and an Energetic Particle Sensor (EPS)/High Energy Proton and Alpha Detector (HEPAD). The Magnetic Field Sensor (MFS) allows for the real-time determination of the magnitude and orientation of the magnetic field. Data will be telemetered twice a second for magnetic fields having a magnitude of ± 1000 nanotesla (nT). The Solar X-Ray Sensor permits real-time determination of the solar x-ray emission in two spectral bands: 0.5-5 angstroms and 1-8 angstroms. The EPS makes flux measurements of protons in the 0.8 to 500 MeV range. The HEPAD monitors protons in four energy ranges above 350 MeV and alpha particles in two energy ranges above 640 MeV/nucleon.

The 5-minute averaged GOES-9/SEM electron data (>2 MeV) cover the period 03/1995 to the present.

1.1.2.3 Description of the data base

The data base created for the TREND-4 study contains the following quantities:

1. spacecraft ephemeris;
2. spacecraft B,L ;
3. omnidirectional electron flux >2 MeV.

The GOES data base has been plotted as monthly survey plots.

1.1.2 The Meteosat-3/SEM-2 spacecraft and instrument

1.1.2.1 Description of Meteosat-3

Meteosat P2 was a refurbished prototype of Meteosat 2. In general, the spacecraft design, instrumentation, and operation were similar to SMS/GOES (SMS: Synchronous Meteorological Satellite). The spin-stabilized, geostationary spacecraft carried (1) a visible-IR radiometer to provide high-quality, day/night cloud-cover data and to take radiance temperatures of the Earth/Atmosphere system; (2) a meteorological data collection system to disseminate image data to user stations, to collect data from various earth-based platforms, and to relay data from polar-orbiting satellites; (3) a LASSO retro-reflector; and (4) an SEM-2 electron spectrometer, provided by LANL (Los Alamos National Laboratories), to investigate the link between deep dielectric charging and the spacecraft anomalies seen on Meteosat 1 and 2. The cylindrically shaped spacecraft measured 210 cm in diameter and 430 cm in length, including the apogee boost motor. The primary structural members were an equipment platform and a central tube. The radiometer telescope was mounted on the equipment platform and viewed the Earth through a special aperture in the side of the spacecraft. A support structure extended radially out from the

central tube and was affixed to the solar panels, which formed the outer walls of the spacecraft and provided the primary source of electrical power. Located in the annulus-shaped space between the central tube and the solar panels were station-keeping and dynamics control equipment and batteries. Proper spacecraft attitude and spin rate (approximately parallel to the Earth's spin axis and approximately 100 rpm) were maintained by jet thrusters mounted on the spacecraft and activated by ground command. The spacecraft used both UHF-band and S-band frequencies in its telemetry and command systems. A lower power VHF transponder provided telemetry and command during launch and then served as a backup for the primary subsystem once the spacecraft attained synchronous orbit.

The Meteosat-3 satellite was launched on 15/06/1988, and decommissioned in November 1995. The satellite longitude varied between 0° and -75°; (see Fig. 1.2).

1.1.2.2 Description of the Space Environment Monitor

The data used in this study was measured by the SEM-2 Space Environment Monitor. The objective of this instrument was to investigate the link between the spacecraft anomalies (as experienced previously on Meteosat F1 and F2) and deep dielectric charging by energetic electrons. The sensor unit was an SEM-2 Lo-E sensor provided by LANL as a spare from other programs. The instrument is identical to the Low Energy Electron unit on the Energetic Particle Detector, flown on the Defense Support Program series of satellites. The electronics and the calibration of the instrument were provided by MSSL. The instrument contained five surface barrier detector-collimator systems, oriented at polar angles of 30, 60, 90, 120, and 150 deg relative to the spacecraft spin vector, which was approximately parallel to the Earth's spin axis. Each collimator covered a nominal 10 degrees full angle. Each system measured electrons in 5 energy channels between 43 and 300 keV. In 100 sec, full energy and azimuthal coverage was obtained, for a particular polar angle. In 5 successive 100 sec intervals, the full latitudinal coverage was also obtained. A Memory Upset Monitor was also included, looking for single event upset errors in a known memory pattern in the memory of a test RAM. A brief description of the instrument and a discussion of the results may be found in the paper by Coates et al. (1989). The sensor design was described by Aiello et al. (1975).

1.1.2.3 Description of the data base

The data base created for the TREND-4 study contains the following quantities:

1. spacecraft ephemeris;
2. spacecraft B,L ;
3. omnidirectional electron flux in 5 channels: 201.8-300 keV, 134.9-201.8 keV, 90.7-134.9 keV, 59.4-90.7 keV, 42.9-59.4 keV;
4. spectral index: the slope of the logarithm of the energy spectrum, calculated using a least squares fit;
5. anisotropy index: describes the angular shape of the plasma distribution relative to its axis of symmetry.

The whole data base has been plotted as monthly survey plots.

1.1.3 The CRRES/MEA spacecraft and instrument

1.1.3.1 Description of CRRES

The Combined Release and Radiation Effects Satellite (CRRES) was launched into a geosynchronous transfer orbit (GTO) for a nominal three-year mission to investigate fields, plasmas, and energetic particles inside the Earth's magnetosphere. As part of the CRRES program the SPACERAD (Space Radiation Effects) project, managed by Air Force Geophysics Laboratory, investigated the radiation environment of the inner and outer radiation belts and measured radiation effects on state-of-the-art microelectronics devices. Other magnetospheric, ionospheric, and cosmic ray experiments were also included onboard CRRES and supported by NASA or the Office of Naval Research. The chemical release project was managed by NASA/MSFC (Marshall Space Flight Center) and utilized the release of chemicals from onboard canisters at low altitudes near dawn and dusk perigee times and at high altitudes near local midnight. The chemical releases were monitored with optical and radar instrumentation by ground-based observers to measure the bulk properties and movement of the expanding clouds of photo-ionized plasma along field lines after the releases occurred. In order to study the magnetosphere at different local times during the mission, the satellite orbit was designed to precess with respect to the Earth-Sun line such that the local time at apogee decreased by 2.5 minutes/day from 08:00 (LT) just after launch and returned to this position in nineteen month cycles. The CRRES spacecraft had the shape of an octagonal prism with solar arrays on the top side. The prism is 1 m high and 3 m between opposite faces. Four of the eight compartments were for the chemical canisters and the other four housed the SPACERAD and other experiments. The spacecraft body was spun at 2.2 rpm about a spin axis in the ecliptic plane and kept pointed about 12 degrees ahead of the Sun's apparent motion in celestial coordinates. Pre-launch and in-flight operations were supported by the Space Test and Transportation Program Office of the U.S. Air Force Space Division. Contact with the CRRES spacecraft was lost on 12/10/1991 and was presumed to be due to onboard battery failure.

1.1.3.2 Description of the Space Environment Monitor

The Medium Electron Sensor, also called MEA or Sensor A, was one of the two parts of the Medium Energy Electron Spectrometer and measured the temporal, spectral, and directional variations of the electron fluxes at approximate energies of 100-2000 keV (Vampola et al., 1992). This sensor consisted of a 0.085 T magnet assembly, a tungsten collimator, 18 lithium-drifted solid-state detectors placed in the focal plane of the 180 degree focusing magnet, shielding, Indox V pole pieces, and both internal and external disk-loaded collimators. The internal collimators prevented scattered particles from being measured and, along with the external collimators, defined the acceptance angle for the instrument. The acceptance angle in the horizontal direction (parallel to the pole piece faces) was +/-11 degrees and independent of energy. In the vertical direction the angle varied with energy; it was +/-11 degrees for the lowest energy channel (46.8-107 keV) and dropped to +/-3 degrees for the highest energy channel (2100-2200 keV). The 15 energy channels between these extremes provided a Delta-E/E starting at about 0.5 and decreased with energy to about 0.06. The final counter was shielded to provide a background measurement for protons and bremsstrahlung. The geometric factors, in units of mm² sr keV, varied with energy, starting at 4.74 for the first, or lowest, energy channel, peaking at 5.67 for the third energy channel, and falling monotonically to 2.15 for the highest energy channel. The aperture was perpendicular to the spin axis of the spacecraft with the horizontal direction pointing along the spin axis. This experiment was part of the SPACERAD project sponsored by AFGL.

1.1.3.3 Description of the data base

The data base created for the TREND-4 study contains the following quantities:

1. spacecraft ephemeris;
2. spacecraft B,L ;
3. differential perpendicular electron flux in 17 channels (0.123-1.714 MeV).

The CRRES/MEA data base has been plotted as two-weekly survey plots.

1.1.4 The STRV1b/REM spacecraft and instrument

1.1.4.1 Description of STRV1b

On 17/06/1994 the Space Technology Research Vehicle (STRV-1B) with a Radiation Environment Monitor (REM) aboard was launched with an Ariane rocket. The orbit of the STRV satellite is highly elliptical with apogee and perigee altitude of 300 km and 36000 km, respectively and a period of ~10 hours. Its inclination in respect to the Earth equator is 7° (GTO). The GTO passes repeatedly through the earth radiation belts and is an excellent orbit for studying the radiation environment through a range of altitudes.

1.1.4.2 The Radiation Environment Monitor (REM)

The REM detector consists of two thin (300 μm thick), totally depleted silicon diodes, measuring the differential linear energy transfer (LET) of charged particles. The detector electronics measures the energy deposit and increments one of 16 counters. Data is accumulated over a period of typically 100 seconds and then stored as a 16-bin histogram. The two detectors differ in size (150 mm^2 and 50 mm^2) and shielding. Both detectors are covered with a spherical dome of 3 mm Al and the larger detector with additional 0.75 mm Ta. Whereas the first detector sees protons as well as electrons (called e-detector) the extra tantalum of the second detector reduces the penetration for electrons in the relevant energy range (2 - 10 MeV) by approximately a factor of 200 and makes this detector better at monitoring protons (energy range 35 - 300 MeV) (called p-detector). Due to the variation of the energy loss of protons in silicon in this energy range the incident energy of the protons is measured, whereas the incident energy of the detected electrons is only poorly determined.

1.1.4.3 Description of the data base

The data base created for the TREND-4 study contains the following quantities:

1. spacecraft ephemeris;
2. spacecraft B,L ;
3. differential omnidirectional electron flux in 3 channels: 1.0-2.2 MeV, 2.2-4.6 MeV, 4.6-10.0 MeV.

The STRV1b/REM data base has been plotted as two-weekly survey plots.

1.1.5 The MIR/REM spacecraft and instrument

1.1.5.1 Description of MIR

Russia's Mir Space Station has been in orbit for over 12 years. The first element of the station was launched on 20/02/1986 at an inclination of 51.6°;. The current Mir Space Station is actually a complex of different modules that have been pieced together. The MIR station orbits the earth every 90 minutes on a nearly circular orbit (inclination 52°;) at an altitude of ~400km.

The Mir module, the first module of the complex placed in orbit, is the main module of the station. It provides docking ports for the other modules to attach to. There are five docking ports on the transfer compartment of the Mir module. One along the long axis of the module, and 4 along the radius in 90 degree increments. There is another docking port on the aft end of the Mir module. The various modules that are attached to the docking ports can be moved around to different configurations.

In the middle of September 1994, a second REM (the first being on STRV 1b) was shipped to the Russian manned MIR station and was subsequently mounted on the outside of the space station by one of the cosmonauts.

1.1.4.2 The Radiation Environment Monitor (REM)

The REM detector consists of two thin (300 mm thick), totally depleted silicon diodes, measuring the differential linear energy transfer (LET) of charged particles. The detector electronics measures the energy deposit and increments one of 16 counters. Data is accumulated over a period of typically 100 seconds and then stored as a 16-bin histogram. The two detectors differ in size (150 mm² and 50 mm²) and shielding. Both detectors are covered with a spherical dome of 3 mm Al and the larger detector with additional 0.75 mm Ta. Whereas the first detector sees protons as well as electrons (called e-detector) the extra tantalum of the second detector reduces the penetration for electrons in the relevant energy range (2 - 10 MeV) by approximately a factor of 200 and makes this detector better at monitoring protons (energy range 35 - 300 MeV) (called p-detector). Due to the variation of the energy loss of protons in silicon in this energy range the incident energy of the protons is measured, whereas the incident energy of the detected electrons is only poorly determined.

1.1.4.3 Description of the data base

The data base created for the TREND-4 study contains the following quantities:

1. spacecraft ephemeris;
2. spacecraft B, L ;
3. dose behind two shieldings.

The STRV1b/REM data base has been plotted as two-weekly survey plots.

1.1.6 ISEE-1 And ISEE-2

Data from the WIM and KED instruments onboard ISEE-1 and ISEE-2, respectively, are available from the TREND-3 study. The data from ISEE-1 is very sparse, and therefore not suited for the present study. The data coverage from ISEE-2 is better, but due to its very eccentric orbit, the radiation belts are traversed very quickly, and hence the coverage is not

sufficient for a time analysis. Therefore, it was decided not to use the ISEE data in this context. The ISEE-2 data base has been plotted as monthly survey plots.

1.2 Selection of the periods of interest

The main selection criterion was the availability of data from satellite missions overlapping in time. For the data available in this study, three such periods have been identified. They are indicated by the dash-dot boxes in Fig. 1.1, and will be called A, B, and C in increasing order of time.

From these periods, a number of two-week intervals have been selected on the basis of the criteria described below. For each of the two-week intervals, combination plots have been produced that show data from different instruments in the same plot.

The main driving parameter of Salammbô is the planetary index K_p . Therefore, we based the selection of periods on the ten day history of K_p . Three states of the magnetosphere were defined:

1. quiet: K_p stayed low during the ten preceding days;
2. diffusion: K_p stayed between 4 and 6 during the ten preceding days;
3. injection: K_p exceeded 7 at least once during the ten preceding days.

The behaviour of other indices during the same time periods was used to further select from the cases conform to the above selection criteria. In addition, several other periods were selected for other reasons, which are discussed in the relevant sections. In the end, eight cases have been retained for the Salammbô runs.

1.2.1 Period A: 1 Jan 86 - 2 Mar 87

1.2.2 Period B: 16 May 90 - 30 Nov 91

1.2.3 Period C: 1 Apr 94 - 31 Dec 95

1.2.1 Period A: 1 Jan 86 - 2 Mar 87

Figure 1.3 shows the ten day history of K_p for period A. Additional indices for this period are shown in Figure 1.4. Three two-week periods were selected (see Table 1.1), two on the basis of the K_p history, and one because it falls in the CDAW-9 campaign. Unfortunately, ISEE-2 data for these periods (and, on closer inspection, for the whole of Period A) are either missing or too sparse, so that in the end Period A was dropped from the study.

Table 1.1 Overview of the two-week periods.

Period	Type	Status
6-18 Feb 86	Injection	Rejected: Sparse ISEE-2 data
30 Apr - 12 May 86	Double storm (CDAW-9)	Rejected: No ISEE-2 data
25 Jun - 7 Jul 87	Quiet	Rejected: Sparse ISEE-2 data

1.2.2 Period B: 16 May 90 - 30 Nov 91

Figure 1.5 shows the ten day history of K_p for period A. Additional indices for this period are

shown in Figure 1.6. Eight preliminary two-week periods were selected (see Table 1.2). Of these eight, four were retained for a detailed study (indicated by a link in Table 1.2).

Table 1.2 Overview of the two-week periods.

Period	Type	Status
30 Jul - 11 Aug 90	Minor storm, followed by continuous decrease in fluxes	Retained
20 Aug - 1 Sep 90	Multiple K_P peaks	Rejected: limited response in GOES and Meteosat data
8-20 Oct 90	Typical storm plus diffusion period	Retained
28 Oct - 9 Nov 90	Successive K_P peaks, related to D_{st} decrease and solar wind velocity increase, respectively	Retained
15-27 Nov 90	Quiet period	Rejected: limited response in GOES data
26 Nov - 8 Dec 90	D_{st} Decrease, followed by rapid decrease of K_P	Rejected: no response in GOES data
12-24 Dec 90	Quiet period	Rejected: limited response in GOES and Meteosat data, problems with CRRES
23 Jan - 4 Feb 91	K_P Increases with different responses	Rejected: sparse CRRES coverage
4-16 Mar 91	Quiet period	Rejected: no Meteosat data
22 Mar - 3 Apr 91	Major storm	Rejected: no Meteosat data
2-14 May 91	Quiet period between K_P increases	Rejected
24 Sep - 6 Oct 91	Period of diffusion followed by storm	Retained

1.2.3 Period C: 1 Apr 94 - 31 Dec 95

Figure 1.7 shows the ten day history of K_P for period A. Additional indices for this period are shown in Figure 1.8. Fifteen preliminary two-week periods were selected (see Table 1.3). Of these fifteen, five were retained for a detailed study (indicated by a link in Table 1.3).

Table 1.3 Overview of the two-week periods.

Period	Type	Status
4-16 Apr 94	Long period of diffusion	Rejected: no STRV or MIR data
19 Jun - 1 Jul 94	Quiet period, followed by K_P increase	Rejected: no STRV or MIR data
16-28 Jul 94	Quiet period	Rejected: no STRV or MIR data
1-12 Oct 94	Injection, followed by diffusion	Rejected: very sparse STRV and MIR data
27 Oct - 7 Nov 94	Injection	Rejected: no STRV or MIR data during the injection period
17-29 Jan 95	Two minor storms separated by quiet period	Rejected: very limited response in the measured fluxes
28 Jan - 8 Feb 95	Two minor storms separated by diffusion period	Rejected: no GOES-8 and sparse MIR data
3-15 Mar 95	Storm without increase in GOES or Meteosat fluxes	Retained
25 Mar - 6 Apr 95	Successive storms, studied by Desorgher et al. (1997, 1998)	Retained
5-17 Apr 95	Storm with very high, sustained GOES and Meteosat fluxes	Retained
28 May - 14 Jun 95	Strong increase of GOES and STRV fluxes, followed by very long decrease of GOES and Meteosat fluxes	Retained
3-15 Jul 95	Very quiet period	Rejected: no Meteosat or MIR data
5-17 Sep 95	Fluctuating K_P	Rejected: sparse STRV and MIR data
26 Sep - 8 Oct 95	Injection	Rejected: no STRV data after injection, no MIR data

References

Aiello, W. P., et al., IEEE Trans. Nucl. Sci., NS-22, p. 575, 1975.

Baker, D. N., R. L. McPherron, T. E. Cayton, and R. W. Klebesadel, Linear Prediction Filter Analysis of Relativistic Electron Properties at 6.6 Re, JGR, 95, No. A9, pp. 15133-15140, 1990

Coates, A. J., et al., Proceedings of the Spacecraft Charging Technology Conference (Monterey, CA, 1989) (NSSDC Tech. Ref. File B39329)

Desorgher, L., P. Bühler, A. Zehnder, E. Daly, L. Adams, Outer radiation belt losses during magnetic storm, Workshop Space Radiation Environment Modelling: New Phenomena and Approaches, Moscow (Russia), October 7-9, 1997

Desorgher, L., P. Bühler, E. Fluckiger, A. Zehnder, E. Daly, L. Adams, Modelling of the outer electron belt during magnetic storms, 32nd COSPAR Scientific Assembly, Nagoya (Japan), 12-19 July, 1998

Vampola, A.L., Osborn, J.V., Johnson, B.M., CRRES Magnetic Electron Spectrometer AFGL-701-5A (MEA), J. Spacecr. \ Rockets, 29, 592-595, 1992

List of figures

Figure 1.1

Time coverage of the missions from which data were used in the study.

Figure 1.2

Evolution of the Meteosat-3 longitude.

Figure 1.3

Ten-day history of K_p for Period A.

Figure 1.4

Indices for Period A.

Figure 1.5

Ten-day history of K_p for Period B.

Figure 1.6

Indices for Period B.

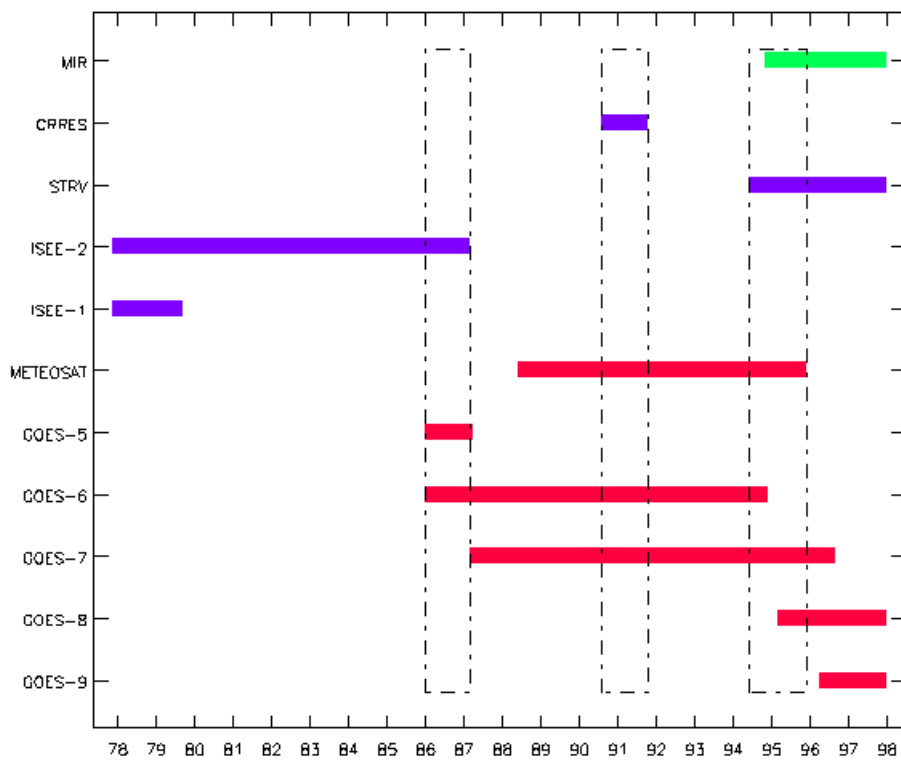
Figure 1.7

Ten-day history of K_p for Period C.

Figure 1.8

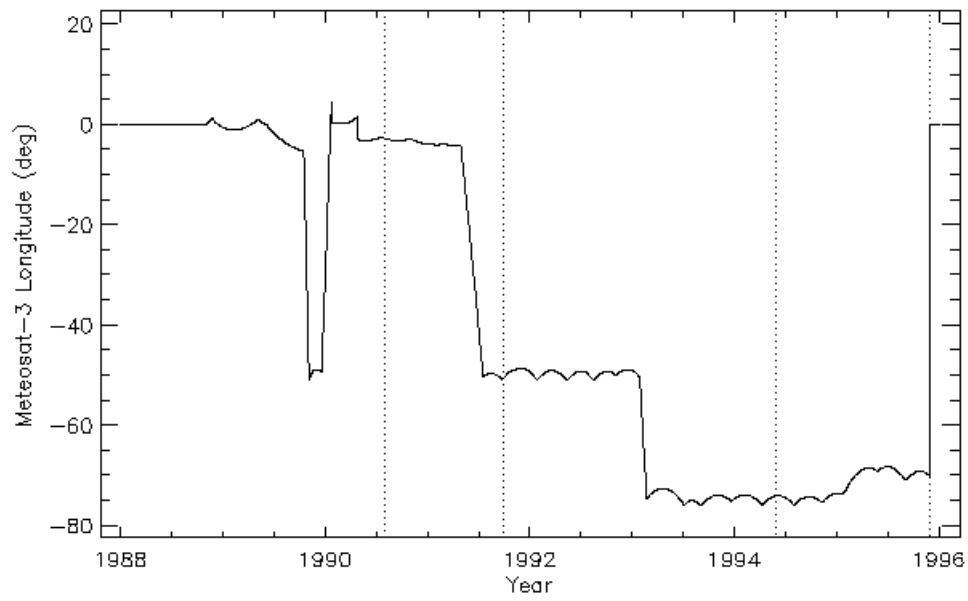
Indices for Period C.

Figure 1.1



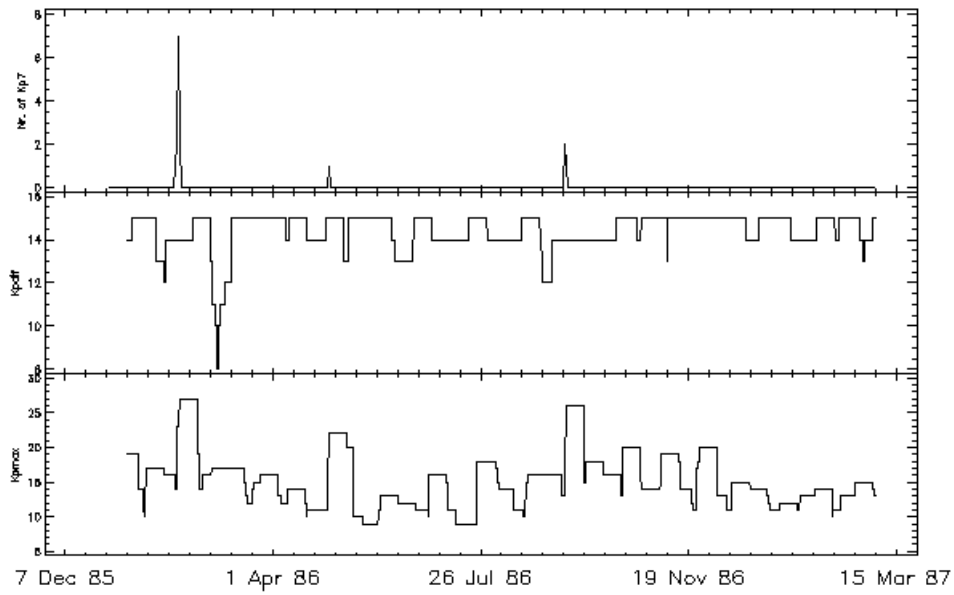
Time coverage of the missions from which data were used in the study. The colour code has the following meaning: green for low altitude missions, purple for HEO orbits, and red for GEO orbits.

Figure 1.2



Evolution of the Meteosat-3 longitude. The vertical dotted lines indicate the periods of interest selected for the TREND-4 study.

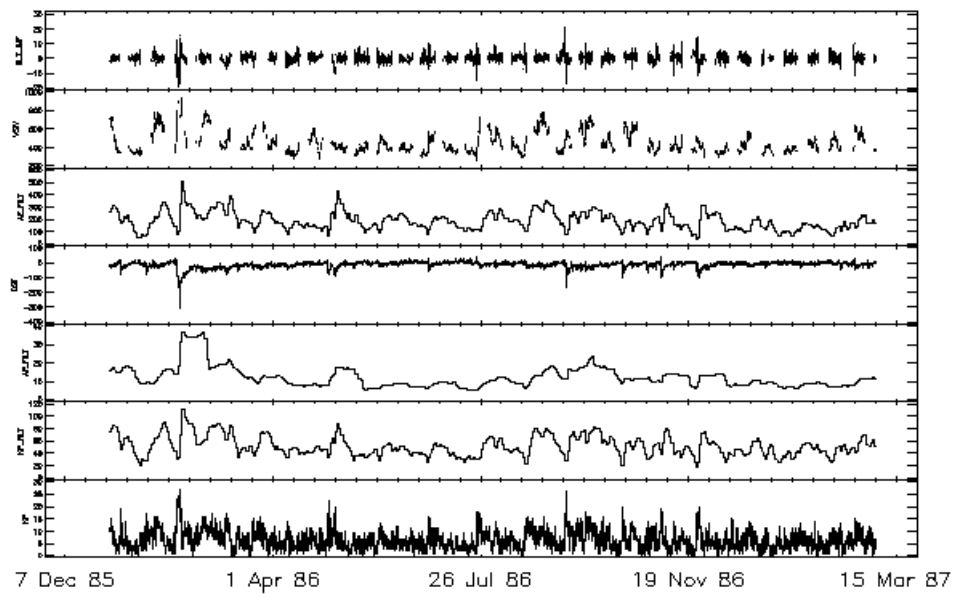
Figure 1.3



Ten-day history of K_p for Period A. The three panels (counting from the top) show:

1. the number of times K_p exceeded 7 over the preceding ten days;
2. the maximum value (times 3) of $|K_p - 5|$ over the preceding ten days;
3. the maximum value (times 3) of K_p over the preceding ten days.

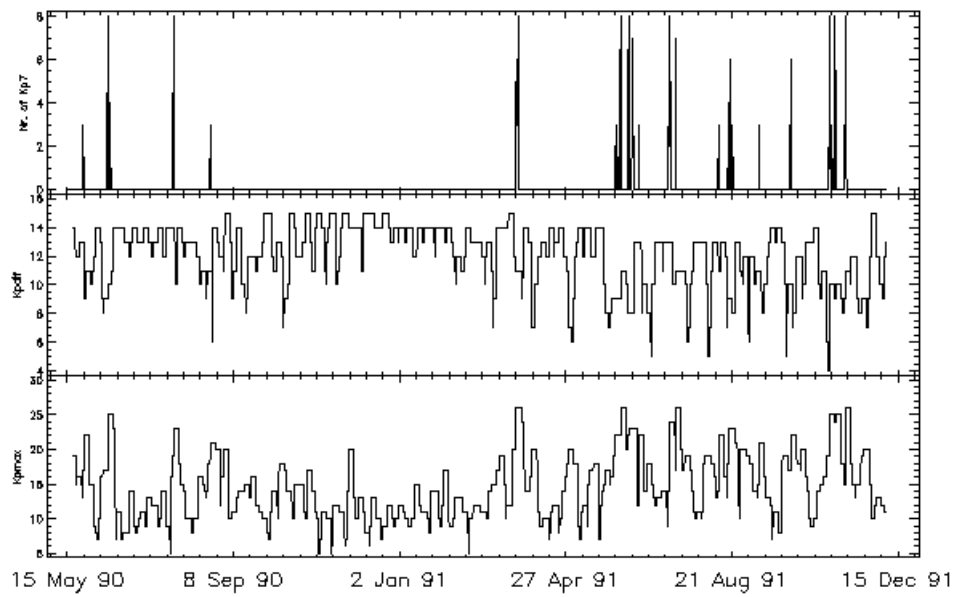
Figure 1.4



Indices for Period A (from the top down):

1. $B_{Z,IMF}$
2. solar wind velocity
3. filtered AE (Baker et al., 1990)
4. D_{st}
5. A_p averaged over the preceding fifteen days;
6. filtered K_p (Baker et al., 1990)
7. K_p

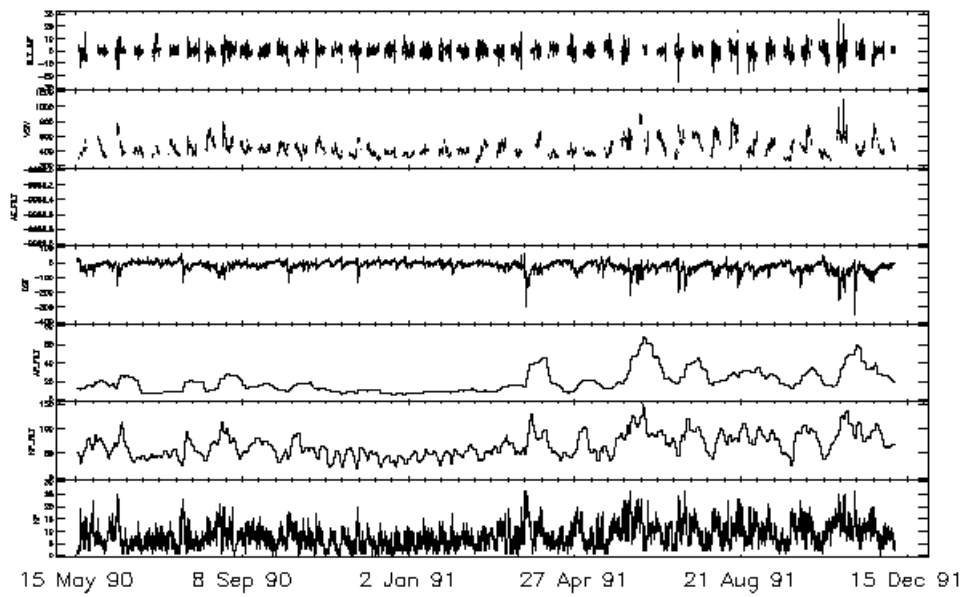
Figure 1.5



Ten-day history of K_p for Period B. The three panels (counting from the top) show:

1. the number of times K_p exceeded 7 over the preceding ten days;
2. the maximum value (times 3) of $|K_p - 5|$ over the preceding ten days;
3. the maximum value (times 3) of K_p over the preceding ten days.

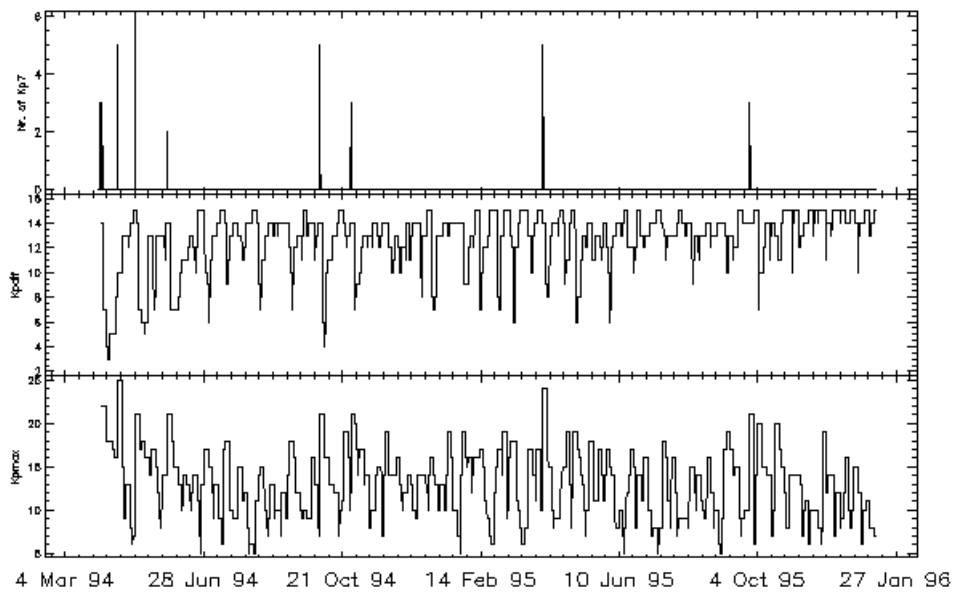
Figure 1.6



Indices for Period B (from the top down):

1. $B_{Z,IMF}$
2. solar wind velocity
3. filtered AE (Baker et al., 1990)
4. D_{st}
5. A_p averaged over the preceding fifteen days;
6. filtered K_p (Baker et al., 1990)
7. K_p

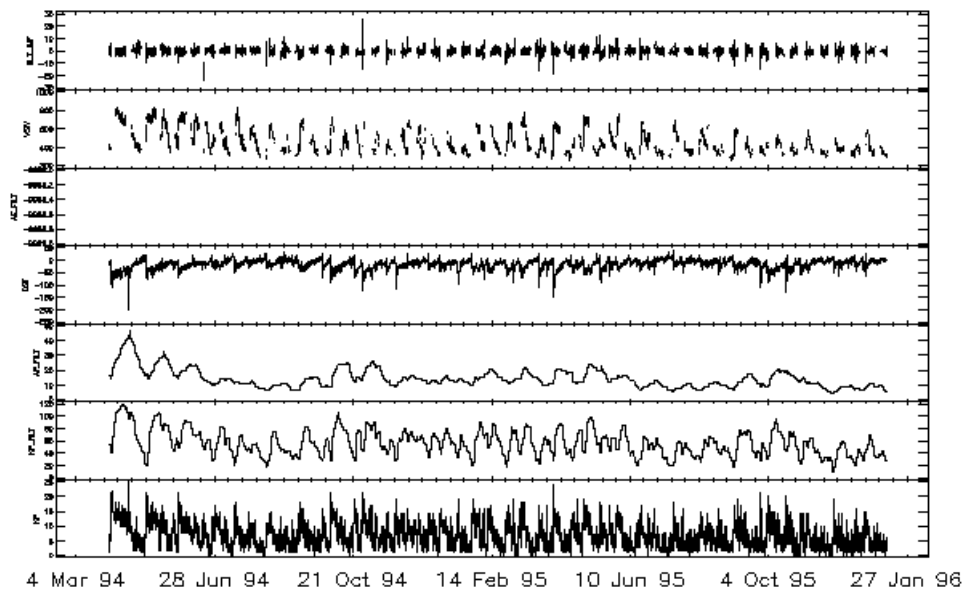
Figure 1.7



Ten-day history of K_p for Period C. The three panels (counting from the top) show:

1. the number of times K_p exceeded 7 over the preceding ten days;
2. the maximum value (times 3) of $|K_p - 5|$ over the preceding ten days;
3. the maximum value (times 3) of K_p over the preceding ten days.

Figure 1.8



Indices for Period C (from the top down):

1. $B_{Z,IMF}$
2. solar wind velocity
3. filtered AE (Baker et al., 1990)
4. D_{st}
5. A_p averaged over the preceding fifteen days;
6. filtered K_p (Baker et al., 1990)
7. K_p